

Measurement based FHSS–type Drone Controller Detection at 2.4GHz: An STFT Approach

Batuhan Kaplan^{*†}, İbrahim Kahraman^{*‡}, Ali Görçin^{*§}, Hakan Ali Çırpan[†], Ali Rıza Ekti^{*¶}

^{*} Informatics and Information Security Research Center (BİLGEM), TÜBİTAK, Kocaeli, Turkey

[†] Department of Electronics and Communication Engineering, İstanbul Technical University, İstanbul, Turkey

[‡] Department of Electrical and Electronics Engineering, Boğaziçi University, İstanbul, Turkey

[§] Faculty of Electronics and Communications Engineering, Yıldız Technical University, İstanbul, Turkey

[¶] Department of Electrical and Electronics Engineering, Balıkesir University, Balıkesir, Turkey

Emails: batuhan.kaplan@tubitak.gov.tr, ibrahim.kahraman@boun.edu.tr, agorcin@yildiz.edu.tr, hakan.cirpan@itu.edu.tr, arekti@balikesir.edu.tr

Abstract—The applications of the unmanned aerial vehicles (UAVs) increase rapidly in everyday life, thus detecting the UAVs and/or its pilot is a crucial task. Many UAVs adopt frequency hopping spread spectrum (FHSS) technology to efficiently and securely communicate with their radio controllers (RCs) where the signal follows a hopping pattern to prevent harmful interference. In order to realistically distinguish the frequency hopping (FH) RC signals, one should consider the real–world radio propagation environment since many UAVs communicate with RCs from a far distance in which signal faces both slow and fast fading phenomenons. Therefore, in this study different from the literature, we consider a system that works under real–conditions by capturing over–the–air signals at hilly terrain suburban environments in the presence of foliage. We adopt the short–time Fourier transform (STFT) approach to capture the hopping sequence of each signal. Furthermore, time guards associated with each hopping sequence are calculated using the autocorrelation function (ACF) of the STFT which results in differentiating the each UAV RC signal accurately. In order to validate the performance of the proposed method, the results of normalized mean square error (MSE) respect to different signal–to–noise ratio (SNR), window size and Tx–Rx separation values are given.

Index Terms—short–time Fourier transform, frequency hopping, UAV remote controller detection

I. INTRODUCTION

Unmanned aerial vehicles (UAVs) have become a prevalent part of the daily life with their applications to many fields such as mapping and surveying, transportation, surveillance, law enforcement, aerial imaging and agriculture [1]. Besides the aforementioned use of UAVs in many areas, one should keep in mind that UAVs can also be used dangerously to create unwanted incidents especially when they are diverted to the sensitive airspace near airports and their presence may cause accidents which can result in fatal crashes [2]. Moreover, UAVs can be utilized for

collecting information about people, organisations, and companies without their consent. Therefore, identification of UAV systems and their communication are great importance, especially to prevent unwanted situations. In this context, it is known that most of the communication between the UAVs and wireless radio controller (RC) utilize the spread spectrum technology of frequency hopping spread spectrum (FHSS) on industrial, scientific, and medical (ISM) band at 2.4GHz [3]. Therefore a method to detect and classify these kinds of signals in this band would lead to the identification of the communication between the UAV and the controller.

In literature, most well known FHSS signal detection methods adopt the time–frequency analysis and wavelet analysis [4–7]. It is shown that Wigner Ville distribution, Wavelet transform method, and array signal processing methods can be used to identify FHSS signals with the burden of heavy computational complexity which make them hard to satisfy the real–time implementation. Since short–time Fourier transform (STFT) based detection method does not need any prior information about received signal compared to computationally complex algorithms, STFT becomes the designated optimum detector in the absence of information regarding the received signal [8]. However, one should note that in order to achieve good results with STFT, signal–to–noise ratio (SNR) value needs to be high. Thus, in this study, we propose STFT based blind signal detection method for FHSS UAV RC signals by using over–the–air signal measurements which accounts for the signal imperfections present in the nature of real–world conditions (e.g. fading, multipath, and so on) by considering the hilly terrain suburban environments in the presence of foliage. Furthermore, the literature utilizes the simulated data instead of over–the–air signals in general and these simulations assume that there is no time guards between hops. This assumption makes differentiation of

frequency hopping (FH) signals easier, however, many hopping signals use time guards and also these time guards are different for different signal sources. The proposed approach is also able to detect the time guards between each hopping sequence using the autocorrelation function (ACF) [9] of the STFT which results in differentiating the each drone RC signal accurately.

The paper is organized as follows, Section II details the system model. Section III presents the proposed method. The measurement setup is explained in Section IV. In Section V, measurement results are given and discussed. Finally, Section VI concludes the paper.

II. SIGNAL MODEL

Drone controller signals might be FH signals that have temporal statistical characteristics and they can be written as [6],

$$x(t) = s(t) \sum_{m=0}^{M-1} e^{j2\pi f_{c_m} t_m + \theta_m} \quad (1)$$

where θ_m and f_{c_m} are the carrier phase and carrier frequency of m_{th} hop, respectively. Also, $s(t)$ denotes the complex baseband equivalent of the information bearer for $t \in [0, T]$, M stands for the total number of hop of a signal, t_m is the duration time of m_{th} hop that might be a uniform distribution or not.

The received controller signal which is complex baseband equivalent of the received passband signal and can be expressed as,

$$r(t) = \sum_{n=0}^{N-1} y_n(t) + n(t) + I(t) \quad (2)$$

where $y_n(t)$ is an n_{th} FH signal source, $n(t)$ denotes the complex Additive White Gaussian Noise (AWGN) in which I and Q components are i.i.d with $\mathcal{N}(0, \sigma^2)$, $I(t)$ stands for the interference signal.

A. Short-Time Fourier Transform

STFT approach is utilized to analyze the FH signals as a method to observe the frequency content of this type of non-stationary signals over time. Mathematical expression of STFT of the time-domain signal $z(t)$ can be written as [8],

$$STFT\{z(t)\} = \int_{-\infty}^{\infty} [z(t)w(t-\tau)]e^{-j2\pi f\tau} d\tau \quad (3)$$

where $w(t)$ is the window function. The STFT matrix $S = [s_1[f], s_2[f], \dots, s_K[f]]$ such that i_{th} element of this matrix is a column vector determined by discrete Fourier transform of $r[n]w[n-iR]$,

$$s_i[f] = \sum_{n=0}^{N-1} r[n]w[n-iR]e^{-j2\pi fn} \quad (4)$$

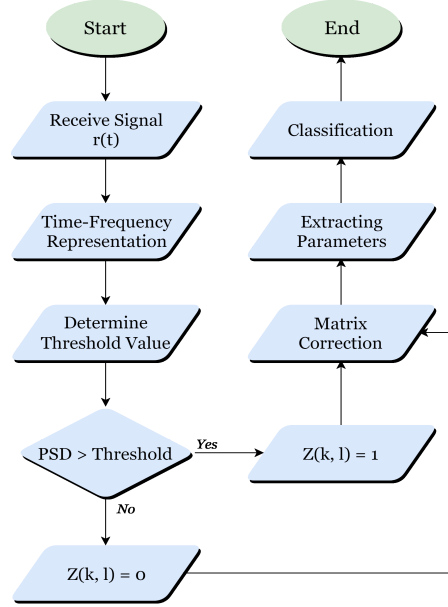


Fig. 1. The flowchart of the proposed detection method.

where $r[n]$ is sampled version of $r(t)$ by considering the anti-aliasing property and R denotes the shifting length.

One should keep in mind that adjusting the time and frequency resolution is crucial point for STFT analysis [10] due to the trade off between them. The length of the time point can be calculated as [11]

$$m = \left\lfloor \frac{N_x - L}{M - L} \right\rfloor \quad (5)$$

where N_x is length of the signal, L denotes the number of overlap in the Fourier transform, M represents the window size, $\lfloor \cdot \rfloor$ stands for the floor operator.

III. PROPOSED METHOD

The received controller signal, $r(t)$, analyzed by STFT method. As depicted in Fig. 1, the flow graph explains how the system works in brief. After the signal is received in the first stage, optimal window time length is decided to get the optimum resolution at (5) based on maximizing the number of elements on the matrix S in the second stage of the flowchart. STFT is calculated in a dBm unit according to power spectral density (PSD) in the same step.

A binarization process is conducted at the following steps of the flowchart; the STFT matrix is converted to a binarized matrix, $Z(k, l)$, with the utilization of a threshold μ . Also, in the flowchart PSD refers to each point in the STFT matrix. Based on the dynamically calculated threshold value, whether the signal presents or not is decided. Therefore, the problem statement can be indicated as the identification of the presence of the unknown FH signal. When the signal is present, $Z(k, l)$ is evaluated as 1 and the new binarized matrix, $Z(k, l)$, is given as,

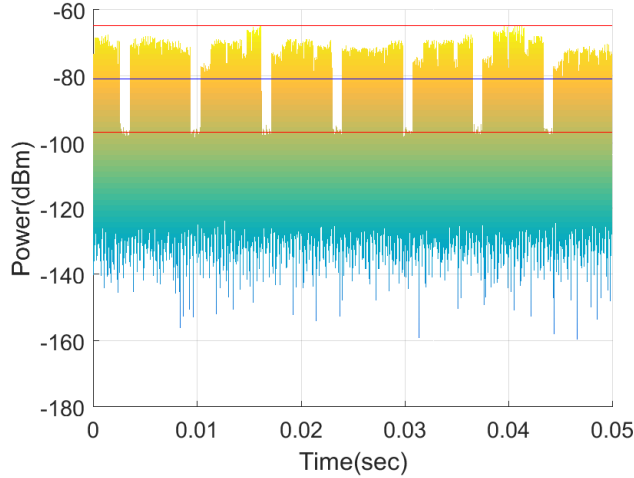


Fig. 2. Estimated threshold representation with S_{max} and $\sigma_{20\%}$ values over real recorded signal.

$$Z(k, l) = \begin{cases} 1, & S(k, l) \geq \mu \\ 0, & S(k, l) < \mu \end{cases} \quad (6)$$

To determine the threshold value, each element of STFT matrix are concatenated and a sorting algorithm implemented to list the power levels of each point of the STFT matrix in a ascending order. Then, we assume that the majority of the received signal comprise of noise, therefore, we take the mean value of the top 20% of the sorted values of STFT matrix to determine a lower bound for the computation of the threshold. Thus, the threshold is calculated as

$$\mu = \frac{S_{max} + \sigma_{20\%}}{2} \quad (7)$$

where S_{max} is the maximum value of the STFT matrix, $\sigma_{20\%}$ denotes the mean of the top 20% samples. Fig. 2 shows S_{max} , $\sigma_{20\%}$, and the threshold value. Please note that even for the very low SNR regimes, the measurement results indicate the feasibility of this threshold selection process.

Due to the wireless impairments on the received signal, some portions of the Z matrix might be missing as shown in Fig. 3(a). In order to represent the signal in a more plausible way, we adopt a widely used morphological dilation and erosion processes from the domain of image processing [12, 13] to recover the received signal properly. A signal with impairments and the output of dilation and erosion processes are shown in Fig. 3.

After the recovery process, it becomes possible to extract the signal parameters such as start time, stop time, center frequency and difference between start time and stop time (dwell time) accurately. The parameter estimation algorithm is given in Algorithm 1. This process is implemented to the Z matrix and the parameters of each signal in the spectrum are extracted. The algorithm simply

Algorithm 1: Parameter Extraction Algorithm

Input: $Z(k, l)$
Output: start time, stop time, center frequency, dwell time, bandwidth

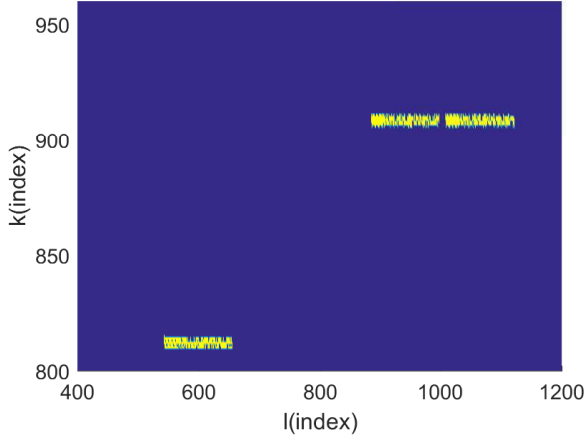
```

1 for  $i \leftarrow 1$  to row do
2   for  $j \leftarrow 1$  to column do
3     count  $\leftarrow 0$ 
4     bandwidth  $\leftarrow 0$ 
5     if  $Z(i, j) == 1$  then
6       start time  $\leftarrow j$ 
7        $f_{start} \leftarrow i$ 
8       while  $Z(i, j) == 1$  do
9         count  $\leftarrow$  count + 1
10         $j \leftarrow j + 1$ 
11       while  $Z(i, j - 1) == 1$  do
12         bandwidth  $\leftarrow$  bandwidth + 1
13          $i \leftarrow i + 1$ 
14       stop time  $\leftarrow j - 1$ 
15        $f_{stop} \leftarrow i - 1$ 
16       center frequency  $\leftarrow \frac{f_{start} + f_{stop}}{2}$ 
17       dwell time  $\leftarrow$  count
Assign 0 to rectangle that founded above.
```

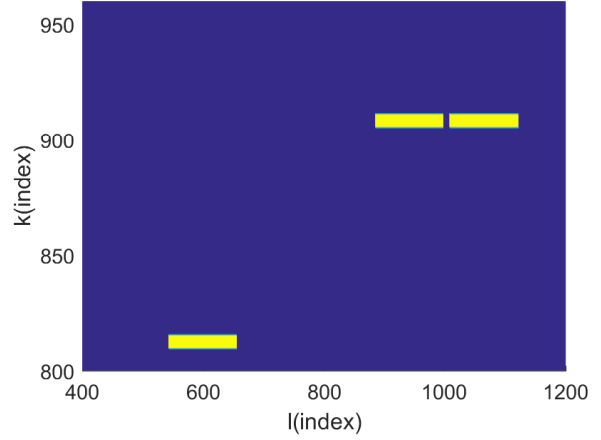
detects the signals from Z and extracts the duration of each independent transmission which can be part of same or different signal sources.

In the last step of the flowchart, controlling for each hop is done to decide whether it belongs to FH signal or not. Due to the signal structure which will be explained in Section IV, time guards are inserted during hopping and this makes classification complicated. Time guards may lead to miss matches between hops because there can be some other signals between them and these miss matches should be corrected. In this paper ACF is utilized for this purpose since the highest correlation peaks occur as the signal matches itself perfectly and this is the case for drone controller FH signals based on the fact that time and frequency characteristics are fixed. ACF is used on Z matrix and result of ACF gives the highest peak at T_1 , which is the fundamental period (6.8ms) for the particular drone controller FH signal. The rest of the peaks give information in regards to hops which are generated from the same source. Thus, we define a set $T = \{T_1, T_2, \dots, T_n\}$ which represents the locations of all the peak values where $T_1 = \sup T$. In other words, we put all the local extremum for interval $(0, T_1)$ to the set T as shown in Fig. 4 meaning that we obtained all the required T values (guard and dwell times) to track and classify hops. Finally, the signal classification block in the flowchart is executed by the procedure: $\exists T_i \in T$ and any two hops, hop_a and hop_b , are emitted from the same signal source if

$$\text{start time}(hop_a) - \text{start time}(hop_b) \equiv T_i \pmod{T_1} \quad (8)$$



(a) Recorded FH drone controller signal with channel impairments.



(b) FH drone controller signal after correction.

Fig. 3. Result of dilation process.

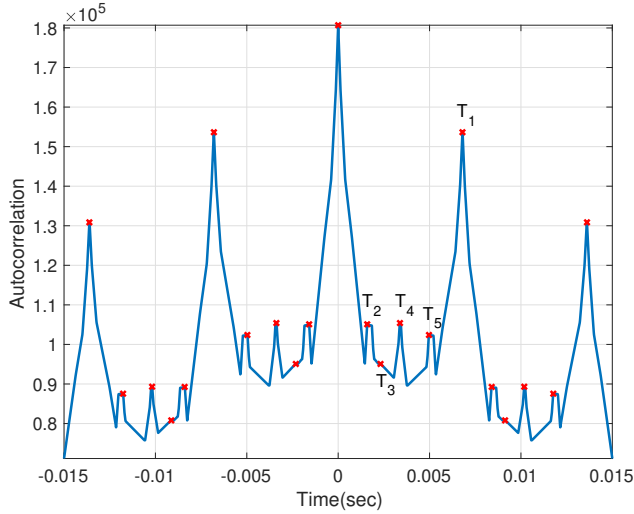


Fig. 4. Time difference estimation between hops utilizing auto correlation function.



Fig. 5. The aerial map of data collection locations.

where start time is the estimated parameter from Algorithm 1. Thus, hop separation is also possible with the proposed method. Please note that even though the method is applied to a particular set of FH signals, it can be utilized to detect any kinds of FH signal with observable time and frequency domain hopping pattern.

IV. MEASUREMENT SETUP

Experimental setup for FH signal parameter estimation is performed in Scientific and Technological Research Council of Turkey (TÜBİTAK) Informatics and Information Security Research Center (BİLGEM). Data collection of FH signal is conducted with different distances from 5m to 135m with 10m intervals between each step. Fig. 5 shows the fixed location of our receiver and locations of the drone controller (transmitter).

A. Hardware Setup

The testbed used in the data acquisition procedure consists of signal source (drone controller) and spectrum analyzer to record the signals.

Futaba T8J RC is used during the experiment as a FH signal source. Futaba T8J RC operates in the 2.4 gigahertz (GHz) ISM band over the half of the spectrum band (up to 2.45 GHz). When analyzing the signal, it is discovered that the RC transmitter is behaved differently compared to the standard FH communication systems (e.g. Bluetooth). An illustration of the periodic hopping sequence for the Futaba T8J RC is shown in Fig. 6. Also, in the figure for τ_{dwell} represents dwell time and fundamental period becomes

$$\Delta t_1 < \Delta t_2 < \Delta t_3 \quad (9)$$

$$3\tau_{dwell} + \Delta t_1 + \Delta t_2 + \Delta t_3 = T_1 = 0.0068sec \quad (10)$$

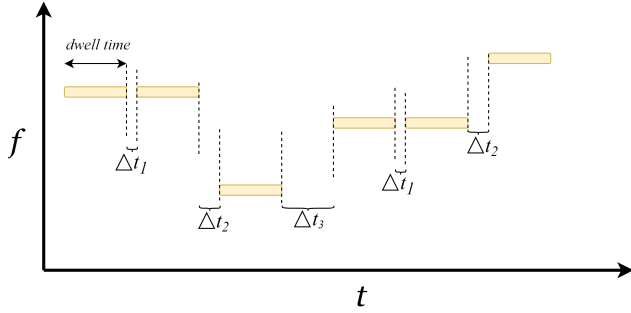


Fig. 6. The hopping pattern of Drone controller signal: Futaba T8J RC as signal source.

TABLE I
FH SIGNAL CHARACTERISTICS

<i>FH Signal</i>	
<i>Dwell Time</i>	1.44ms
<i>Center Frequency Set</i>	2.4GHz-2.45GHz interval
<i>Hopping Sequence</i>	f1 f1 f2 f3 f3 f4 ...

The parameters of Futaba T8J RC FH signal source are listed in Table I. In the receiver side, Rohde&Schwarz FSW 26 signal and spectrum analyzer (SSA) is utilized to record FH signals. SSA can support the frequency range from 2 hertz (Hz) to 26.5GHz. The device provides real-time spectral analysis up to 160 megahertz (MHz) bandwidth. The signals are recorded over the 2.4GHz ISM spectrum band with an omnidirectional antenna.

B. Experimental Procedures

In data collection from real-world, it is assumed that transmitter operates between 2.4GHz-2.48GHz ISM spectrum band. The center frequency of SSA is set to 2.44GHz and bandwidth of interest is adjusted to 80MHz for the purpose of full coverage. Also, SSA is connected to external computer via an Ethernet cable in favor of achieving data storage with ease. The sampling rate depends on the analysis bandwidth of real-time spectrum which is selected as 80MS/s. Each measurement is captured as an I/Q samples and collected 20M I/Q samples during 250ms. However, considering the processing limit, the collected data is divided into pieces with each has 4M samples. Each divided data was considered when calculating the performance of the proposed method. Finally, captured I/Q data is fed into the computer which runs MATLAB R2015b software.

V. MEASUREMENT RESULTS

Over-the-air data collection is realized and the performance of time-frequency analysis method is evaluated. Please note that all the captured data includes real-world propagation effects such as multipath fading, interference, carrier frequency offset (CFO). Fig. 7 shows how overtheair recorded FH signal source behaves during

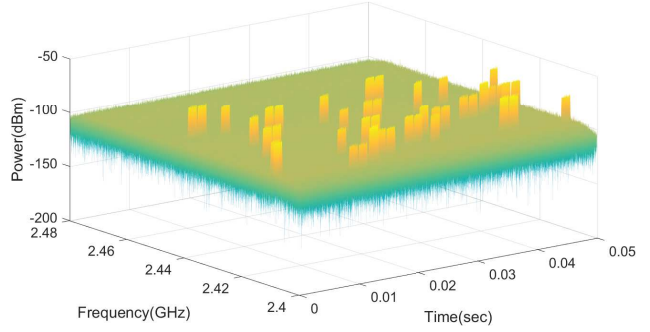


Fig. 7. Recorded 2.4GHz spectrum that comprised of drone controller FH signals.

TABLE II
ESTIMATED PARAMETERS OF FH SIGNAL

<i>Start Time (ms)</i>	<i>Stop Time (ms)</i>	<i>Dwell Time (ms)</i>	<i>Center Frequency (GHz)</i>
1.7930	3.2403	1.4472	2.4271
5.1742	6.6086	1.4344	2.4414
6.7623	8.1967	1.4344	2.4414
8.6066	10.0410	1.4344	2.4211
11.9749	13.4221	1.4472	2.4039

the observation time. Please also note that some of the estimated parameters of the real signal which measured at 25m distance with 5dB SNR can be found in Table II.

In order to validate the performance of the system, normalized mean square error (NMSE) was considered. Normalized MSE can be calculated as [14]

$$NMSE = \frac{1}{N} \sum_{i=1}^N \left(\frac{\hat{t}_i - t}{t} \right)^2 \quad (11)$$

where \hat{t}_i is the estimated hopping time of i_{th} hop and t denotes the true value of hopping time. N represents the total number of hop that must be found. When calculating the error, it is assumed that N equals to 22 in the observation time. Also, 0 values have been added to extracted parameters if there is some undetected signal.

The error curve of an estimated hopping time from measured data is plotted in Fig. 8. In here, error values are determined for three different SNR values and distances. It is clearly seen that as the distance increases, the error of estimation increases. Also poor SNR condition adversely affects the performance. Moreover, even with the same SNR condition, there may be a missing hop of an FH signal in the signal received from the farther point.

As discussed before, another important issue is selection of window size (M). In this regard, precision of window size is also studied. It can be seen that window size directly affects the accuracy of the estimation. While window size decreases, we get high resolution in time but low resolution in frequency. In contrast, increasing window size implies high resolution in frequency but low resolution in

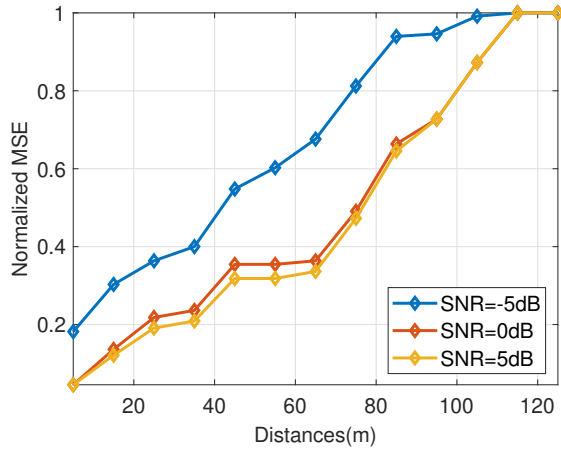


Fig. 8. Estimated hopping time errors vs. distance in terms of normalized MSE.

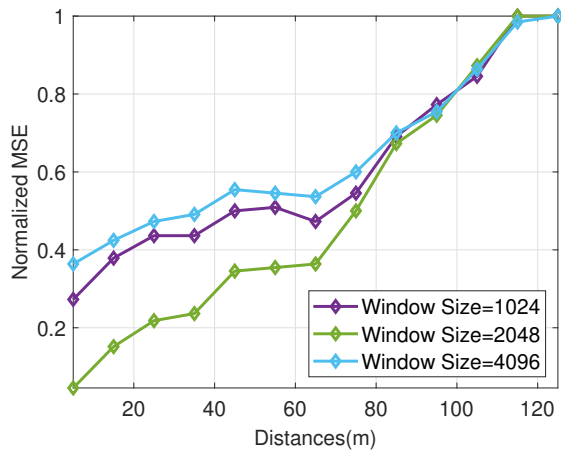


Fig. 9. Estimated hopping time errors vs. distance for different window sizes and for SNR = 0 dB.

time. Because both the frequency and time information are main features to classify the hopping signals, there should be some optimum window size providing better performance. It is empirically shown in Fig. 9 that the optimum window size for STFT is $M = 2048$.

Since the previous works utilize STFT only for deciding whether a signal is hopping between different frequencies, ACF is applied only in time-domain for the signals with no guard times, and the simulations were considered instead of measurements, comparison of the performance of the proposed method with these simulations are avoided in this work.

VI. CONCLUDING REMARKS AND FUTURE DIRECTIONS

In this work, an FH drone controller signal detection algorithm is proposed and the performance of the algorithm is evaluated using measurements of UAV RC in real-world wireless environment. The algorithm can estimate

the guards of the each hopping sequence successfully by using the ACF of STFT, which also leads to the accurate identification whether a FH signal is present or not. The performance of the proposed method is also quantified by normalized MSE for over-the-air signal which are recorded at different distances and SNRs. Measurement results show that reasonable input parameters will improve the performance of frequency hopping signal parameter estimation. In future studies, we will consider adopting the recently emerging deep learning algorithms to distinguish multiple standard based wireless hopping signals.

VII. ACKNOWLEDGEMENT

This publication was made possible by NPRP12S-0225-190152 from the Qatar National Research Fund (a member of The Qatar Foundation). The statements made herein are solely the responsibility of the author[s].

REFERENCES

- [1] DHL, "DHL launches first commercial drone 'parcelcopter' delivery service," Available: <https://www.theguardian.com/technology/2014/sep/25/german-dhl-launches-first-commercial-drone-delivery-service>, Accessed: Oct. 29, 2019.
- [2] FAA, "Federal Aviation Administration UAS Sightings Report," Available: https://www.faa.gov/uas/resources/public_records/uas_sightings_report/, Accessed: Oct. 29, 2019.
- [3] P. Popovski, H. Yomo, and R. Prasad, "Strategies for adaptive frequency hopping in the unlicensed bands," *IEEE Wireless Communications*, vol. 13, no. 6, pp. 60–67, Dec 2006.
- [4] A. Kanaa and A. Z. Shaameri, "A robust parameter estimation of fhss signals using time-frequency analysis in a non-cooperative environment," *Physical Communication*, vol. 26, pp. 9–20, 2018.
- [5] B. Boashash, *Time-frequency signal analysis and processing: a comprehensive reference*. Academic Press, 2015.
- [6] S. Wei, M. Zhang, G. Wang, X. Sun, L. Zhang, and D. Chen, "Robust multi-frame joint frequency hopping radar waveform parameters estimation under low signal-noise-ratio," *IEEE Access*, 2019.
- [7] X. Zhang, X. Wang, and X.-m. Du, "Blind parameter estimation of frequency-hopping signals based on wavelet transform [j]," *Journal of Circuits and Systems*, vol. 4, 2009.
- [8] X. Ouyang and M. G. Amin, "Short-time fourier transform receiver for nonstationary interference excision in direct sequence spread spectrum communications," *IEEE Trans. Signal Process.*, vol. 49, no. 4, pp. 851–863, 2001.
- [9] C.-D. Chung and A. Polydoros, "Parameter estimation of random fh signals using autocorrelation techniques," *IEEE Trans. Commun.*, vol. 43, no. 2/3/4, pp. 1097–1106, 1995.
- [10] N.-K. Kim and S.-J. Oh, "Comparison of methods for parameter estimation of frequency hopping signals," in *International Conference on Information and Communication Technology Convergence (ICTC)*, 2017, pp. 567–569.
- [11] J. Smith, S. U. C. for Computer Research in Music, Acoustics, and S. U. D. of Music, *Spectral Audio Signal Processing. W3K*, 2011, online book, 2011 edition. [Online]. Available: <https://ccrma.stanford.edu/~jos/sasp/>
- [12] R. M. Haralick, S. R. Sternberg, and X. Zhuang, "Image analysis using mathematical morphology," *IEEE Trans. Pattern Anal. Mach. Intell.*, no. 4, pp. 532–550, 1987.
- [13] L. Luo *et al.*, "Detection of an unknown frequency hopping signal based on image features," in *2nd International Congress on Image and Signal Processing*, 2009, pp. 1–4.
- [14] Y. Ma and Y. Yan, "Blind detection and parameter estimation of single frequency-hopping signal in complex electromagnetic environment," in *2016 Sixth International Conference on Instrumentation & Measurement, Computer, Communication and Control (IMCCC)*, 2016, pp. 370–374.